Gas Clumping in the Outskirts of Galaxy Clusters as seen by STAR-X

Christian Norseth [1], Daniel Wik [1], John ZuHone [2], Eric Miller [3], Marshall Bautz [3]

[1] University of Utah, [2] Harvard & Smithsonian Center for Astrophysics, [3] Kavli Institute for Astrophysics and Space Research - MIT

THE UNIVERSITY OF UTAH

THE UNIVERSITY OF UTAH Department of Physics & Astronomy

Introduction

- Galaxy clusters are the largest gravitationally bound structures in the universe.
- They contain 100s to 1000s of galaxies.
- The Intra-cluster-medium (ICM), a hot gas (~107 K) in between galaxies is detectable in the X-ray range via Bremsstrahlung radiation.
- ICM thermodynamical properties are extremely important for cosmology, i.e., how the universe formed and how it is evolving.
- Entropy in particular is essential to understand the dynamical properties of a cluster, including its evolution.
- Observations have shown unexpected results in derived entropy profiles for clusters.
- Gas clumping, pockets of denser and cooler structure within the ICM may explain this unexpected drop in entropy.
- Clumps have not been directly detected.
- STAR-X may be able to detect these clumps.
- This work simulates observations of clumpy galaxy clusters, as seen by STAR-X.

Bremsstrahlung Radiation

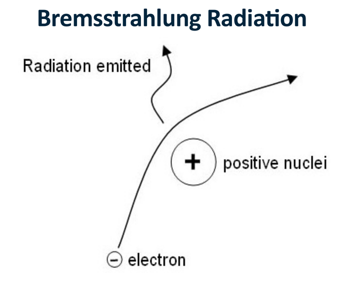

The ICM is so hot that the gas is ionized. When electrons get deflected through interactions with ions, X-ray radiation is produced.

STAR-X

The Survey and Time-domain Astronomical Research eXplorer (STAR-X) is an observatory that was proposed to NASA's most recent Mid-Sized Explorer Class Mission call (MIDEX) at the end of 2021. It is currently one of two missions being considered for selection in 2023. It will have a low particle background due to its low altitude orbit and will be able to better detect faint cluster outskirts, where the Earth's magnetosphere will protect STAR-X from high energy charged particles. It also will be more efficient than previous missions (less exposure time, faster slewing). STAR-X is also designed with a large field of view, large effective area, and an optimum Point-Spread Function (PSF) to minimize noise and gather as much information about a cluster as possible.

Goals

- To reproduce observed entropy profiles using simulated observations and to determine what clumping properties yield observed results.
- To place limits on detectable clump properties (size, temperature, density, number) for STAR-X.

Methods

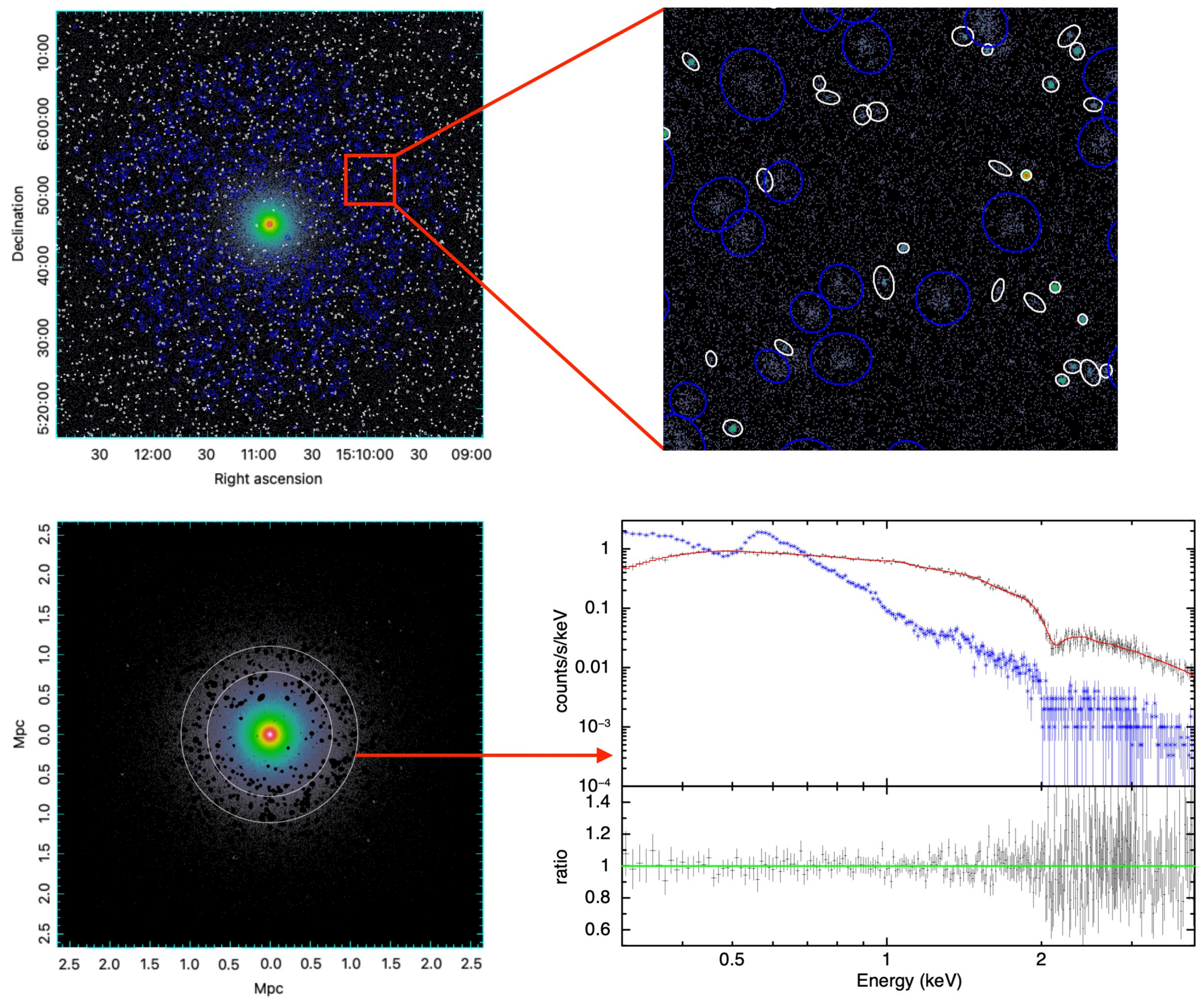

Figure 1: Top Left: Simulated 1 degree observation of clumpy Abell 2029, point sources in white, clumps circled in blue. Top Right: Zoomed-in region of red box in left image. Bottom Left: Smoothed, background-subtracted version of image above with masked point sources and clumps. Both the top and bottom left cluster images are scaled logarithmically and have the same FOV. Bottom Right: Fit of spectrum extracted from Annulus 6, shown in white in bottom left panel. Background-subtracted data are shown in black, The red curve represents the best-fit model, the blue points indicate the background level. The lower panel shows the ratio of the data to the model, indicating the quality of the fit.

Clump Property Analysis:

- Clumps at a given radial size (5kpc - 50kpc) are injected into an empty bounding box with the approximate width of the cluster in question and placed at the cluster's redshift.
- A simulated observation from STAR-X is created including instrumental background and the galactic foreground.
- An attempt at clump detection using *wavdetect* is carried out.
- The density of the clumps are varied until their overall detectability is near either 95% detectable or 5% detectable (see Figure 2 and 3).

Simulation:

Data Grids:

- Two sets of 3D cluster arrays are generated based on a given temperature (Eqn. 1) and density (Eqn. 2) profiles.
- Clumps are randomly "injected" into the arrays with selected properties.
- The datasets are loaded into yt and processed using pyXSIM.

Simulating Photons:

- pyXSIM generates a 3D photon list, based on a thermal source model (apec).
- The output is a 3D array that describes how light would emanate from each cell of the grid based on the temperature and density at that point.

Projecting Photons to Simulate Images:

- The photon list is projected along a line of sight to generate a mock observation of a cluster at a given redshift.
- A 2D event file is then produced.
- Using SOXS, a mock observation is created that simulates the response and background of STAR-X and includes galactic foreground and point sources.

Spectral Analysis:

- Simulated point sources and clumps are identified and masked using *wavdetect*.
- Spectra are extracted from concentric annuli centered at the X-ray emission peak.
- The data is fitted to find temperature and surface brightness values and used to construct radial profiles for temperature and density (see figure 4 and 5).
- An entropy profile can then be derived (Eqn. 3).

Eqn 1: $T_{3D}(r) = T_0 \frac{(\frac{r}{r_t})^{-a}}{(1+(\frac{r}{r_t})^b)^{\frac{c}{b}}} \frac{(\frac{r}{r_{cool}})^{a_{cool}} + \frac{T_{min}}{T_0}}{(\frac{r}{r_{cool}})^{a_{cool}}+1}$

Eqn 2: $n_p n_e = n_0^2 \frac{(r/r_c)^{-\alpha}}{(1+r^2/r_c^2)^{3\beta-\alpha/2}} \frac{1}{(1+r^{\gamma}/{r_s}^{\gamma})^{\varepsilon/\gamma}} + \frac{n_{02}^2}{(1+r^2/r_{c2}^2)^{3\beta_2}}$

Eqn 3: $K = \frac{T}{n^{\frac{2}{3}}}$

Results

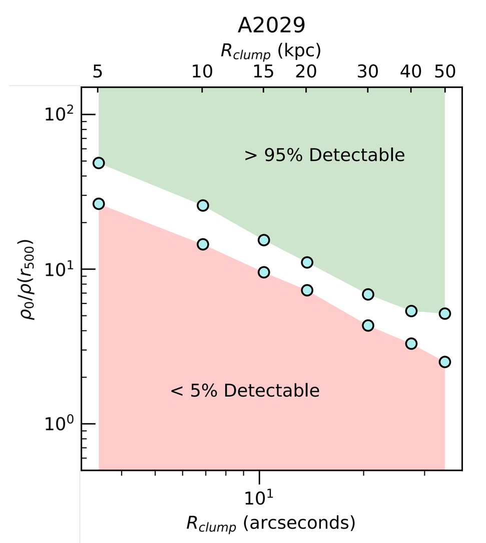

Figure 2: Detectability of gas clumps with a 3.0 keV central temperature within Abell 2029, based on STAR-X's instrumental background and the galactic foreground. The central density of the clumps are scaled by the density at r500 .The green region signifies the parameter space where clumps are extremely likely to be detected by STAR-X, greater than 95% detectable. The red region signifies the parameter space where clumps are extremely unlikely to be detected, less than 5% detectable.

Radius R_{cl} (kpc)	Abell 2029 ρ_0 $(10^{-27}$ g cm$^{-3})$	Number Density $(10^{-8}$ kpc$^{-3})$
5	14.5	6.67
10	7.70	3.52
15	4.60	2.94
20	3.30	1.90
30	2.05	1.61
40	1.60	1.10
50	1.54	0.785

Radius R_{cl} (kpc)	Abell 1246 ρ_0 $(10^{-27}$ g cm$^{-3})$	Number Density $(10^{-8}$ kpc$^{-3})$
5	35.8	2.18
10	15.8	1.34
15	8.95	1.30
20	6.27	1.07
30	4.00	0.667
40	3.05	0.507
50	2.30	0.391

Radius R_{cl} (kpc)	Perseus Cluster ρ_0 $(10^{-27}$ g cm$^{-3})$	Number Density $(10^{-8}$ kpc$^{-3})$
5	5.20	97.0
10	2.81	37.0
15	1.75	21.5
20	1.30	11.4
30	0.90	5.38
40	0.70	4.44
50	0.46	2.98

Figure 3: Detectable limits for gas clumps that recreate observed drops in entropy.

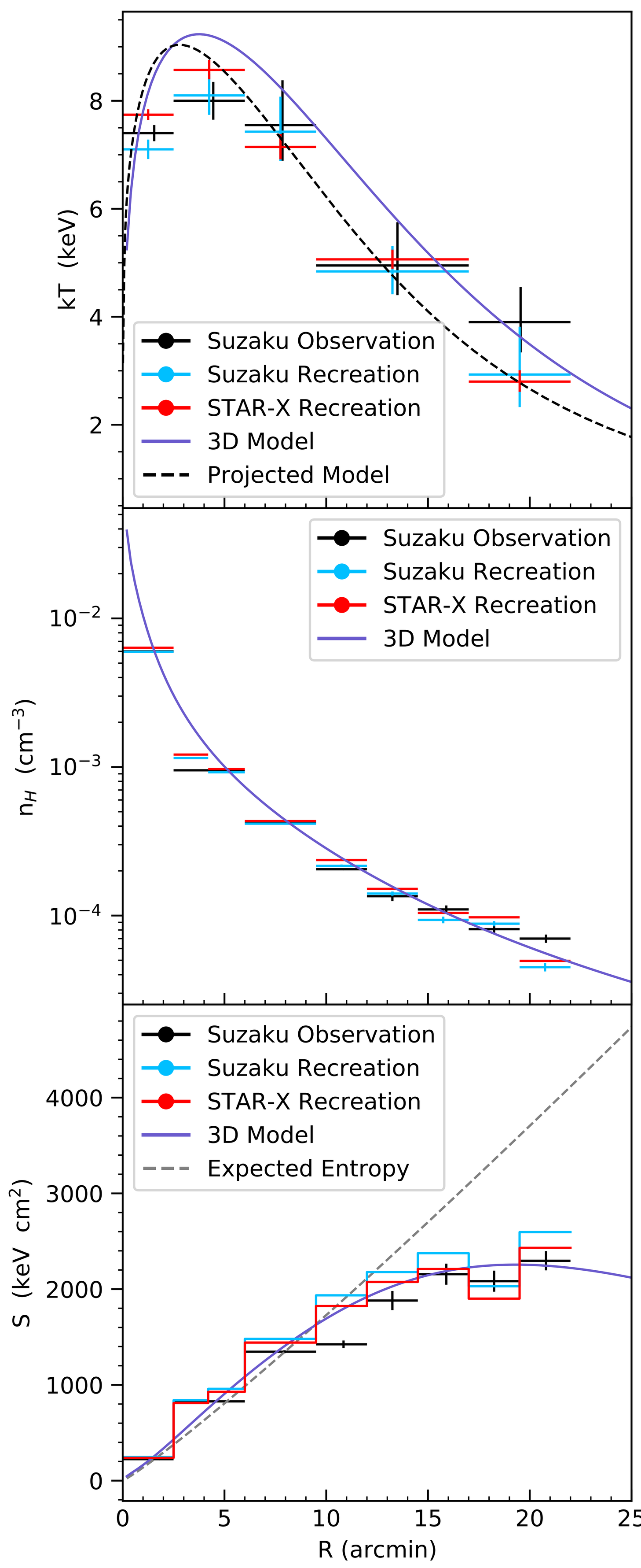

Figure 4: Top: Projected temperatures for Abell 2029 recreations compared to deprojected temperatures from Suzaku observations (Walker et al. 2012b). Dashed black line signifies the projected temperature profile. Middle: Deprojected Hydrogen number density profiles. Bottom: Entropy profiles, dashed grey line signifies the expected entropy (r^1.1) relation. Suzaku observational data is show in black,, a simulated recreation of a Suzaku observation is shown in Blue, and a simulated observation from STAR-X is seen in red. Solid purple lines signify best fit models used to reconstruct cluster.

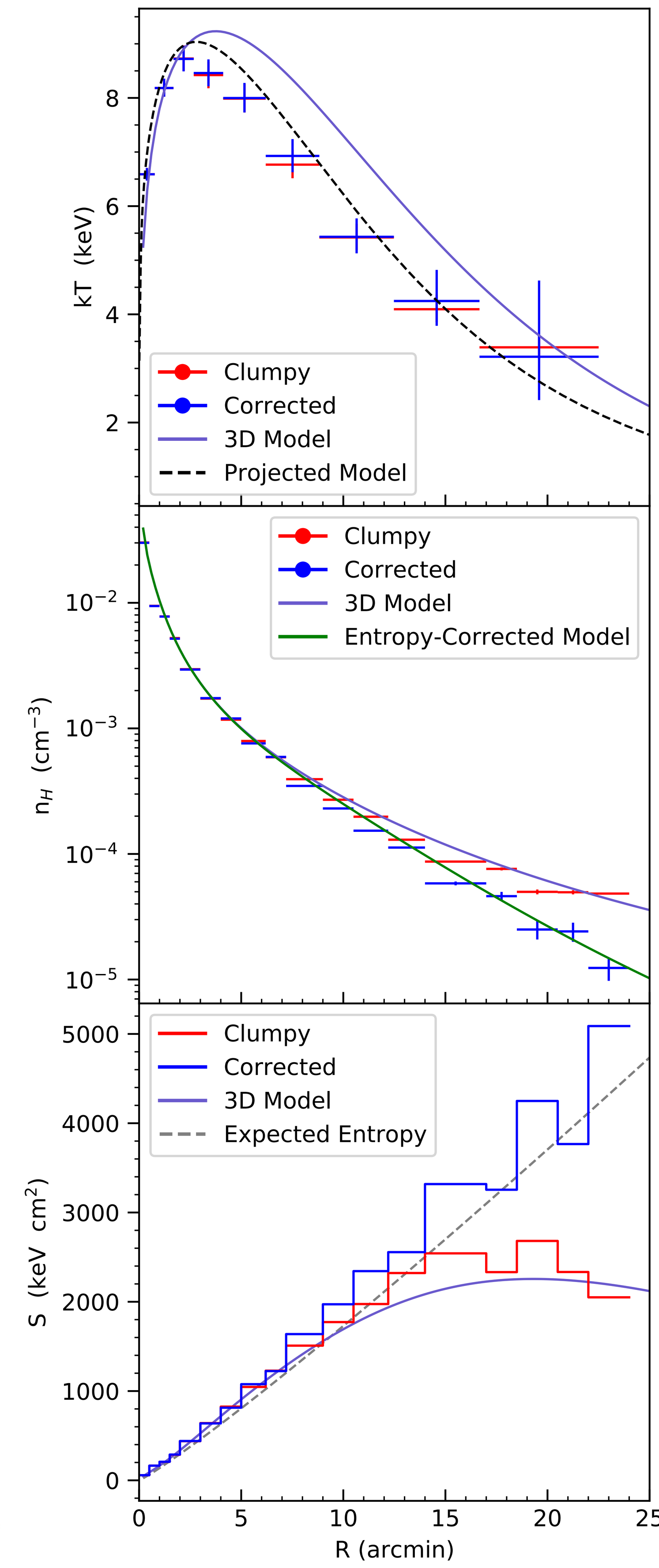

Figure 5: Projected temperatures for an Abell 2029 recreation with clumps injected (red) and clump corrected results (blue). Dashed black line signifies the projected temperature profile. Middle: Deprojected Hydrogen number density profiles for the clumpy A2029 recreation (red) and the clump-corrected results (blue). The green line represents the density profile necessary to yield the expected entropy and was used to construct the cluster. Bottom: Derived entropy profiles for the clumpy A2029 recreation and accompanying clump-correction (blue). Dashed grey line signifies the expected entropy (r1.1) relation. Solid purple lines signify best fit models used to reconstruct cluster.

Discussion

Figure 3:

- A set of detectable clump parameters have been identified.

Figure 4:

- Simulation can produce realistic data.
- The extracted temperature (top), density (middle), and entropy profiles (bottom) from the reconstruction of Abell 2029 for Suzaku (blue) and STAR-X (red) follow the same trends as observational Suzaku data (black).

Figure 5:

- Correcting for clumping (blue) yields the expected entropy profile (bottom, dashed grey).
- Properties for injected clumps that recreate observed drops in entropy are identified.
- The expected entropy profile can be recovered through clump detection within identified clump parameters.

Conclusions

- The primary goal of this research was to determine whether STAR-X would be sensitive enough to detect and mask out gas clumps in the outskirts of galaxy clusters in order to recover entropy profiles of the truly diffuse ICM and to identify detectable gas clump properties.
- Detectable gas clump properties for a range of clump sizes were determined (Figure 2/3).
- Number densities of injected clumps to recreate observed drops in entropy were established (Figure 3/5).
- If clumps are within the range established in Figure 3, STAR-X should be able to detect them.

Future Work

- Identify clump parameters for a wider range of clump temperatures.
- Use cosmological simulations to build more complex clusters.
- Better assess clump feasibility.

References

- Allen, S. W., Evrard, A. E., & Mantz, A. B. 2011, Annual Review of Astronomy and Astrophysics, 49, 409, doi: 10.1146/annurev-astro-081710-102514
- Barcons, X. 2015, Journal of Physics: Conference Series, 610 Bautz, M. W., Miller, E. D., Sanders, J. S., et al. 2009, PASJ, 61, 1117, doi: 10.1093/pasj/61.5.1117
  Biffi, V., Borgani, S., Murante, G., et al. 2016, ApJ, 827, 112, doi: 10.3847/0004-637x/827/2/112
- Cavaliere, A., Lapi, A., & Fusco-Femiano, R. 2011, ApJ, 742, 19, doi: 10.1088/0004-637X/742/1/19
- Eckert, D., Ettori, S., Pointecouteau, E., et al. 2017, Astronomische Nachrichten, 338, 293, doi: 10.1002/asna.201713345
- Eckert, D., Roncarelli, M., Ettori, S., et al. 2015, MNRAS, 447, 2198, doi: 10.1093/mnras/stu2590
- Ghirardini, V., Bulbul, E., Kraft, R., Bayliss, M., & Benson, B. 2021, The Astrophysical Journal, 910, 14, doi: 10.3847/1538-4357/abc68d
- Ichikawa, K., Matsushita, K., Okabe, N., et al. 2013, ApJ, 766, 90, doi: 10.1088/0004-637X/766/2/90
- Lapi, A., Fusco-Femiano, R., & Cavaliere, A. 2010, A&A, 516, A34, doi: 10.1051/0004-6361/201014218
- Lehmer, B. D., Xue, Y. Q., Brandt, W. N., et al. 2012, ApJ, 752, 46, doi: 10.1088/0004-637X/752/1/46
- Morandi, A., & Cui, W. 2013, Monthly Notices of the Royal Astronomical Society, 437, 1909, doi: 10.1093/mnras/stt2021
- Nagai, D., & Lau, E. 2011, ApJ, 731
  Sato, K., Matsushita, K., Yamasaki, N. Y., Sasaki, S., &
- Ohashi, T. 2014, Publications of the Astronomical
- Society of Japan, 66, doi: 10.1093/pasj/psu061 Simionescu, A., Allen, S., Mantz, A., et al. 2011, Science, 6024, 1576, doi: 10.1126/science.1200331
- Urban, O., Simionescu, A., Werner, N., et al. 2013, Monthly Notices of the Royal Astronomical Society, 437, 3939, doi: 10.1093/mnras/stt2209
- Vazza, F., Eckert, D., Simionescu, A., Brüggen, M., & Ettori, S. 2012, Monthly Notices of the Royal Astronomical Society, 429, 799–814, doi: 10.1093/mnras/sts375
- Vikhlinin, A., Kravtsov, A., Forman, W., et al. 2006, ApJ, 640, 691, doi: 10.1086/500288
- Voit, G. M., Kay, S. T., & Bryan, G. L. 2005, MNRAS, 364, 909, doi: 10.1111/j.1365-2966.2005.09621.x
- Walker, S., & Lau, E. 2022, Cluster outskirts and their connection to the cosmic web, arXiv, doi: 10.48550/ARXIV.2202.07056
- Walker, S., Simionescu, A., Nagai, D., et al. 2019, Space Science Reviews, 215, doi: 10.1007/s11214-018-0572-8
- Walker, S. A., Fabian, A. C., Sanders, J. S., & George, M. R. 2012a, Monthly Notices of the Royal Astronomical Society: Letters, 427, L45, doi: 10.1111/j.1745-3933.2012.01342.x
- Walker, S. A., Fabian, A. C., Sanders, J. S., George, M. R., & Tawara, Y. 2012b, Monthly Notices of the Royal Astronomical Society, 422, 3503, doi: 10.1111/j.1365-2966.2012.20860.x
- Zhang, W. W. 2017, in UV, X-Ray, and Gamma-Ray Space Instrumentation for Astronomy XX, ed. O. H. Siegmund, Vol. 10397, International Society for Optics and Photonics (SPIE), 103970O, doi: 10.1117/12.2270862
- Zhuravleva, I., Churazov, E., Arévalo, P., et al. 2015, MNRAS, 450, 4184, doi: 10.1093/mnras/stv900

christian.norseth@gmail.com